

Research Article

RAMRSGL: A Robust Adaptive Multinomial Regression Model for Multicancer Classification

Lei Wang ¹, Juntao Li ², Juanfang Liu ², and Mingming Chang ²

¹Department of Basic Science Teaching, Henan Polytechnic Institute, Nanyang, 473000 Henan, China

²College of Mathematics and Information Science, Henan Normal University, Xixiang, 453007 Henan, China

Correspondence should be addressed to Juntao Li; juntaolimail@126.com and Juanfang Liu; juanfang777@126.com

Received 22 February 2021; Accepted 12 May 2021; Published 26 May 2021

Academic Editor: Lei Chen

Copyright © 2021 Lei Wang et al. This is an open access article distributed under the Creative Commons Attribution License, which permits unrestricted use, distribution, and reproduction in any medium, provided the original work is properly cited.

In view of the challenges of the group Lasso penalty methods for multicancer microarray data analysis, e.g., dividing genes into groups in advance and biological interpretability, we propose a robust adaptive multinomial regression with sparse group Lasso penalty (RAMRSGL) model. By adopting the overlapping clustering strategy, affinity propagation clustering is employed to obtain each cancer gene subtype, which explores the group structure of each cancer subtype and merges the groups of all subtypes. In addition, the data-driven weights based on noise are added to the sparse group Lasso penalty, combining with the multinomial log-likelihood function to perform multiclassification and adaptive group gene selection simultaneously. The experimental results on acute leukemia data verify the effectiveness of the proposed method.

1. Introduction

With the development of technology, the scale of data is constantly increasing, and the dimension of data is rapidly expanding. Data as diverse as transaction data, user rating data, Web usage data, gene expression data, and multimedia data can have hundreds or thousands of dimensions and even more [1]. Therefore, the microarray data has the characteristics of small sample and ultrahigh dimension [2]. The birth of microarray data makes it possible to diagnose complex diseases such as cancer at the genetic level. In the process of using gene expression data for diagnosis, genes are treated as characteristics or attributes, and tissue samples are labeled as specific types, such as tumor tissue or normal tissue, various subtypes of cancer. The classifier is then constructed using machine learning methods to predict the types of the new sample [3–6]. However, only a few genes are closely related to cancer diagnostic tasks for the microarray gene expression data. Therefore, although the classification process is completely consistent with the traditional data, cancer classification based on the gene expression data still faces great challenges [7, 8].

Due to the characteristics of automatic variable selection, sparse regression methods [9–13] have attracted a surge of attention in cancer diagnosis and gene selection. To tackle the problem that the l_1 regularization has a biased gene selection and does not have the oracle property, Wu et al. [13] in 2018 have investigated l_1/l_2 regularized logistic regression for gene selection in high-dimensional cancer classification. In terms of classification performance, the experimental results on three DNA microarray datasets demonstrate that the proposed method outperforms other commonly used sparse methods. To address the problem that there are high correlations among genes, a two-stage sparse logistic regression has been proposed by Algamil and Lee [12] in 2019, which is aimed at obtaining an efficient subset of genes with high classification capabilities by combining the screening approach as a filter method and adaptive Lasso with a new weight as an embedded method. The experimental results demonstrate that the top selected genes are biologically related to the cancer type, which is useful for cancer classification using DNA gene expression data in real clinical practice. To handle the group structures of the time-dependent clinical variables in the model, Zhang et al. [10] in 2020 have developed a high-

dimensional logistic regression and introduced the group spline-penalty or group smooth-penalty. This method is easy to implement since it can be turned into a group minimax concave penalty problem after certain transformations.

Yuan and Lin [14] first proposed a group Lasso regression model using l_2 -norm penalty. Group Lasso [15–17] can generate interpopulation sparsity, i.e., automatic identification of important gene groups. To identify several important genes but not all genes in the same group, Simon et al. [18] proposed the sparse group Lasso. Since both the l_1 -norm penalty and the l_2 -norm penalty are introduced into the model, it can generate both intergroup sparsity and intragroup sparsity. By introducing the weighted gene coexpression network analysis and information theory into the sparse group Lasso, Li et al. [19] proposed three criteria for evaluating the importance of genes within the population and then proposed the adaptive sparse group Lasso model.

Generally, the group Lasso methods rely on early grouping, so it is important to choose an appropriate grouping method. To this end, various algorithms have been proposed. Clustering, the most popular, has been used since the first gene expression dataset is born and is still the most widely used [20, 21]. Furthermore, clustering methods can be divided into four categories: prototype-based clustering [22, 23], density-based clustering [24, 25], hierarchical clustering [26, 27], and spectral clustering [28]. For gene expression data, Sharan et al. [29] proposed a clustering algorithm by linking kernels, which is named CLICK. The CLICK algorithm uses graph theory and statistical techniques to identify tight groups of highly similar elements and then uses some heuristic process to extend kernel extensions into modules. Weighted gene coexpression network analysis (WGCNA) [30] is a clustering method developed for microarray data, which improves the classical bottom-up clustering algorithm. Instead of slicing a tree at a certain height like traditional hierarchical clustering, WGCNA uses a dynamic tree slicing algorithm to ensure that the resulting clustering meets several criteria related to cohesion and separation. Affinity propagation (AP) is a spectral-based clustering algorithm proposed by Frey and Dueck in 2007 [31]. AP clustering takes the similarity measure between data points as input and then automatically identifies a group of high-quality clustering centers and corresponding clusters through the continuous transmission of two kinds of real value information between data points.

It is necessary to construct a robust sparse regression model for high-dimensional data with noise [32–35]. Traditional least square methods may not produce reliable estimators, while the least absolute deviation (LAD) estimator is an effective robust regression method. Wang et al. [36] proposed LAD-Lasso by combining LAD and Lasso, which can not only estimate parameters and select variables at the same time but also has strong resistance to heavy tail error or response outliers. In addition, the parameters of LAD-Lasso are easy to estimate and have oracle properties. However, LAD loss is not applicable for small residuals, especially when there is no heavy tail error and no outliers, the estimator shows poor performance. To improve on that, Lambert-Lacroix and Zwald [37] proposed a robust regression model combining Huber criterion and adaptive Lasso penalty. Huber criterion is also

an effective method of robust regression. It is a mixture of the square error of relatively small error and the absolute error of relatively large error, which makes the model have good performance regardless of the size of residuals. To alleviate the influence of conversion parameters on the performance of Huber Lasso, Zheng et al. [38] proposed a convex combination of adaptive Lasso and LAD-Lasso with data-driven power, namely, robust adaptive Lasso (RA-Lasso).

To solve multiclassification problems effectively, Vincent and Hansen [39] introduced sparse group Lasso penalty into multinomial log-likelihood function, proposed multinomial sparse group Lasso model, and developed the solution algorithm. Due to this model adopts the method of random grouping, the obtained groups are not of biological significance. Li et al. [19] used WGCNA to cluster genes in advance, introduced a clustering method that could better explain the structure of genes, and then proposed an adaptive multinomial regression model with sparse overlap group Lasso penalty. Although these methods [40, 41] can solve the multiclassification problems in cancer diagnosis well, how to build a robust multinomial regression model for noisy data and how to use the noise information to construct data-driven weights so as to further increase the robustness of the model are problems that need to be solved.

In this paper, to obtain biologically significant gene clusters for each cancer subtype, AP clustering is used to cluster the three acute leukemia subtypes in advance on the noise-removed data. Then, the noise matrix is used to construct data-driven weights, based on which an adaptive sparse group Lasso penalty for multicancer microarray data is proposed. Furthermore, a robust adaptive multinomial regression model with sparse group Lasso penalty (RAMRSGGL) is proposed based on log-likelihood loss, and a regularization solution algorithm is developed.

The structure of the rest paper is as follows: in Section 2, we first define the multiclassification problem and then elaborate the RAMRSGGL model. Section 3 verifies the effectiveness of the proposed model through experiments. Section 4 eventually summarizes the whole paper.

2. Problem and Method

2.1. Preliminaries. Since a cancer often has different subtypes, cancer diagnosis requires not only determining whether a patient has cancer but also accurately identifying the type of cancer they have. As a result, cancer diagnosis can be modeled as a multiclassification problem. Suppose cancer has K ($K \geq 3$) subtypes and a gene expression dataset $\mathcal{D} = \{(\mathbf{x}_1, y_1), (\mathbf{x}_2, y_2), \dots, (\mathbf{x}_N, y_N)\}$ contains N samples, where $\mathbf{x}_i \in \mathbb{R}^M$ and $y_i \in \{1, 2, \dots, K\}$ are the gene expression sample and its label, respectively. For notation convenience, let $\mathbf{X} = (\mathbf{x}_1, \mathbf{x}_2, \dots, \mathbf{x}_N)^T$ and $\mathbf{y} = (y_1, y_2, \dots, y_N)^T$ denote the sample matrix and its corresponding label vector, respectively. To identify the type of new sample \mathbf{x} , we need to construct a decision function $f(\mathbf{x})$ with K discriminant functions f_k , i.e.,

$$f(\mathbf{x}) = \arg \max_k f_k(\mathbf{x}). \quad (1)$$

Generally, linear discriminant function $f_k(\mathbf{x}) = \beta^{(k)T} \mathbf{x} + \beta_0^{(k)}$ is most widely used. Therefore, the construction of the decision function is always transformed into the problem of solving the optimal parameters $\beta^{(k)}$ and $\beta_0^{(k)}$ of each discriminant function.

The above regression coefficients can be usually solved by the following Lasso model [42]:

$$\min_{\beta} \frac{1}{2} \|\mathbf{y} - \mathbf{X}\beta\|_2^2 + \lambda \|\beta\|_1, \quad (2)$$

where $\lambda \geq 0$ is the regularization parameter. By using the l_1 -norm penalty, some coefficients that correspond to the features can be reduced to zero. To select features in groups, Yuan and Lin [14] proposed group Lasso (GL) in 2006.

$$\min_{\beta} \frac{1}{2n} \left\| \mathbf{y} - \sum_{l=1}^c \mathbf{X}^{(l)} \beta^{(l)} \right\|_2^2 + \lambda \sum_{l=1}^c \sqrt{m_l} \|\beta^{(l)}\|_2, \quad (3)$$

where $\mathbf{X}^{(l)}$ and $\beta^{(l)}$ are the subset of the l -th group, and m_l represents the number of the l -th group. To generate both intergroup sparsity and intragroup sparsity, Simon et al. proposed sparse group Lasso (SGL) [18] in 2013.

$$\min_{\beta} \frac{1}{2n} \left\| \mathbf{y} - \sum_{l=1}^c \mathbf{X}^{(l)} \beta^{(l)} \right\|_2^2 + (1 - \alpha) \lambda \sum_{l=1}^c \sqrt{m_l} \|\beta^{(l)}\|_2 + \alpha \lambda \|\beta\|_1, \quad (4)$$

where $0 \leq \alpha \leq 1$ is also the regularization parameter. SGL penalty is a convex combination of Lasso penalty and group Lasso penalty, which can achieve two kinds of sparsity simultaneously. To achieve adaptive population gene selection, Li et al. proposed adaptive sparse group Lasso (ASGL-CMI) in 2017.

$$\min_{\beta} \frac{1}{2n} \left\| \mathbf{y} - \sum_{l=1}^c \mathbf{X}^{(l)} \beta^{(l)} \right\|_2^2 + (1 - \alpha) \lambda \sum_{l=1}^c \sqrt{m_l} \|\beta^{(l)}\|_2 + \alpha \lambda \|\mathbf{W}\beta\|_1, \quad (5)$$

where \mathbf{W} is the weight constructed based on information theory. The ASGL-CMI can adaptively select the important genes in the selected population by introducing the weight with biological significance.

The real gene expression datasets often have some missing values and contain noise, while the current models mostly ignore the point. Therefore, this paper is devoted to establish a robust classification model for gene expression data with noise and effectively identify the important genes related to cancer.

2.2. Robust Adaptive Multinomial Regression with Sparse Group Lasso Penalty. First, the input sample matrix is decomposed through robust principal component analysis. Then, the overlapping clustering strategy is adopted to cluster the genes on the leukemia data with noise removed by AP clustering, and the weight is constructed by using the noise matrix. Finally, the RAMRSL model is constructed according to the clustering results and weight.

2.2.1. Robust Principal Component Analysis. It is assumed that the gene expression data \mathbf{X} conforms to the noise distribution, and the noise is usually sparse. As a modification of the widely used statistical procedure of principal component analysis (PCA), the robust principal component analysis (RPCA) works well with respect to grossly corrupted data [43]. Therefore, \mathbf{X} can be decomposed into a low-rank matrix \mathbf{D} and the noise matrix \mathbf{E} using RPCA, i.e.,

$$\begin{aligned} \min_{\mathbf{D}, \mathbf{E}} \quad & \|\mathbf{D}\|_{\hat{a}} + \lambda \|\mathbf{E}\|_1 \\ \text{s.t.} \quad & \mathbf{X} = \mathbf{D} + \mathbf{E}, \end{aligned} \quad (6)$$

where $\|\cdot\|_{\hat{a}} = \sum \sigma(\cdot)$ denotes the nuclear norm, i.e., the sum of its singular values; $\|\cdot\|_1 = \sum |\cdot|$ denotes the l_1 -norm, i.e., the sum of its absolute values. Due to \mathbf{D} represents the clean matrix containing the information of the original data structure and \mathbf{E} represents the sparse noise matrix, both components are of arbitrary magnitude.

2.2.2. Gene Clustering. As a clustering algorithm based on the concept of message passing, affinity propagation (AP) provides a new method to reveal the inter-relationships between genes. Let $s(i, k)$ be a function that quantifies the similarity between any two genes \mathbf{x}_i and \mathbf{x}_k , let $r(i, k)$ be a function that quantifies how well-suited \mathbf{x}_k is to serve as the clustering center for \mathbf{x}_i , relative to other candidate clustering centers for \mathbf{x}_i , and let $a(i, k)$ be a function that quantifies how appropriate it would be for \mathbf{x}_i to pick \mathbf{x}_k as its clustering center, taking into account other points preference for \mathbf{x}_k as a clustering center. According to Frey and Dueck in [31], the algorithm performs the following updates iteratively.

First, responsibility updates are sent around:

$$r(i, k) \leftarrow s(i, k) - \max_{k' \neq k} \left\{ a(i, k') + s(i, k') \right\}. \quad (7)$$

Then, availability is updated as follows:

$$a(i, k) \leftarrow \min \left\{ 0, r(k, k) + \sum_{i' \in \{i, k\}} \max \left\{ 0, r(i', k) \right\} \right\} (i \neq k), \quad (8)$$

$$a(k, k) \leftarrow \sum_{i' \neq k} \max \left\{ 0, r(i', k) \right\}. \quad (9)$$

Iterations are performed until either the cluster boundaries remain unchanged over a number of iterations, or some

Solution algorithm of RAMRSGL.

Input: The sample matrix \mathbf{X} and its label \mathbf{y} .

Output: The optimal coefficients β^* and the predictive label $\hat{\mathbf{y}}$.

1 Obtain \mathbf{D} and \mathbf{E} by decomposing \mathbf{X} ; See Sec. 2.2.1

2 Obtain the expanded matrix $\bar{\mathbf{D}}$ of \mathbf{D} ; See Step 4 in Sec. 2.2.2

3 Construct the weight matrix \mathbf{W} ; See Eq. (14)

4 Divide $\bar{\mathbf{D}}$ into training set $\bar{\mathbf{D}}_{\text{train}}$ and test set $\bar{\mathbf{D}}_{\text{test}}$;

5 foreach $\alpha \leftarrow \{0.2, 0.3, 0.5, 0.8, 0.9\}$ do

6 Fit the RAMRSGL model based on MSGSL toolkit;

7 Obtain the regularization parameter λ by ten-fold cross validation;

8 end

9 Determine the model with the optimal parameter pair (α^*, λ^*) ;

10 Extract the non-zero coefficients β^* of the optimal model and determine the corresponding genes and groups;

11 Obtain the prediction label $\hat{\mathbf{y}}$ of $\bar{\mathbf{D}}_{\text{test}}$ according to Eq. (1);

ALGORITHM 1

predetermined number of iterations is reached. For the data point i , let

$$l = \arg \max_k \{a(i, k) + r(i, k)\}, \quad (10)$$

if $l = i$, then, the data point i can be served as a clustering center; otherwise, the data point l is seen as a clustering center of i . In the implementation of AP clustering, we use negative squared Euclidean distances to measure the similarity, referring to [31] for more details.

Considering that the subtype genes of each cancer may have a specific group structure, the overlapping clustering strategy is adopted, and AP clustering is performed on the data of each cancer to cluster genes. To avoid the influence of noise, the clean data \mathbf{D} obtained by decomposition is grouped, and the specific process is as follows:

Step 1. \mathbf{D}^T is divided into K sub-matrices depending on different sample labels.

Step 2. K symmetric metric matrices are constructed by using Pearson correlation coefficient.

Step 3. Based on the above metric matrices, AP clustering is carried out for each kind of data sample to obtain K group indicator vectors v_1, v_2, \dots, v_K , the corresponding group sequence of the vector elements specified by the gene.

Step 4. Expand the dimension of input matrix \mathbf{D} :

Step 4.1. According to v_1, v_2, \dots, v_K , rearrange the columns of \mathbf{D} , and then get K matrices $\mathbf{D}_1, \mathbf{D}_2, \dots, \mathbf{D}_K$;

Step 4.2. The expanded dimension matrix $\bar{\mathbf{D}} \in \mathbb{R}^{n \times KM}$ is obtained by combining $\mathbf{D}_1, \mathbf{D}_2, \dots, \mathbf{D}_K$ by row.

Step 5. The group index vector \mathbf{v} is constructed according to the specific group sequence in the data matrix after dimensional expansion. Let V denotes the maximum value of \mathbf{v} , i.e., a total of V groups are obtained.

2.2.3. Model Construction. Since each gene is repeated K times in the expanded dimension matrix $\bar{\mathbf{D}}$, to maintain the correspondence between the noise information and the data after dimensional expansion, the noise matrix \mathbf{E} should be expanded accordingly. As such, rearrange the columns of \mathbf{E} according to v_1, v_2, \dots, v_K and then get K matrices $\mathbf{E}_1, \mathbf{E}_2, \dots, \mathbf{E}_K$. The expanded dimension matrix $\bar{\mathbf{E}} \in \mathbb{R}^{n \times KM}$ is obtained by combining $\mathbf{E}_1, \mathbf{E}_2, \dots, \mathbf{E}_K$ by row. Obviously, the more noisy the gene is, the less important it is. Without loss of generality, we use the following gene reliability criterion:

$$s_t^{(l)} = \frac{1}{\|\bar{\mathbf{E}}_t^{(l)}\|_1 + \varepsilon}, \quad t = 1, 2, \dots, K, \quad (11)$$

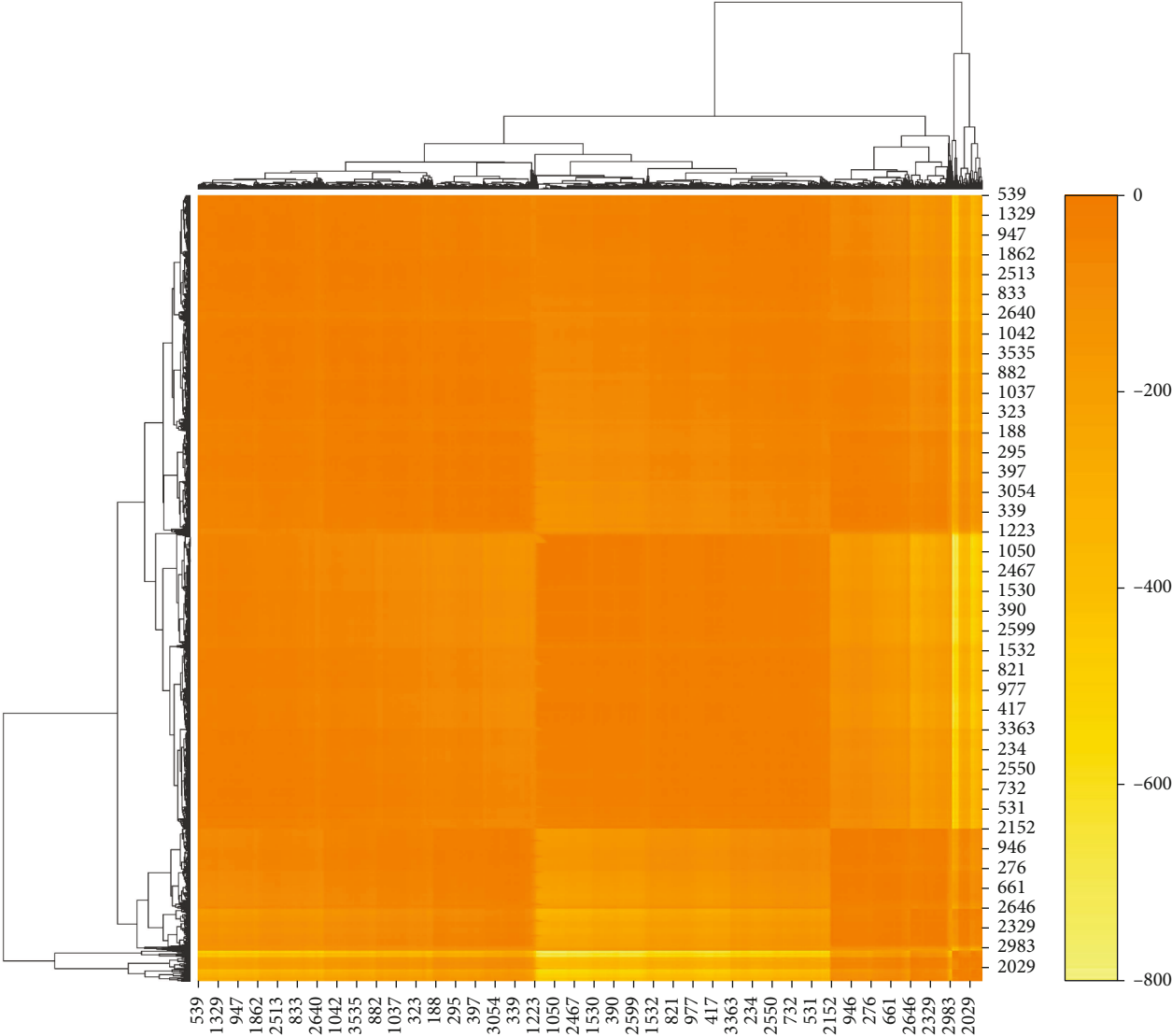
where $s_t^{(l)}$ represents the importance of the t -th gene in the l -th group. According to contraction theory, the regression coefficients of more important genes should be given less weight. Therefore, the weight of the t -th gene in the l -th group can be represented as follows:

$$w_t^{(l)} = \frac{1}{s_t^{(l)}}. \quad (12)$$

Further, the weight vector \mathbf{w} can be obtained.

$$\mathbf{w} = \left(w_1^{(1)} \quad \dots \quad w_{m_1}^{(1)} \quad w_1^{(2)} \quad \dots \quad w_{m_2}^{(2)} \quad \dots \quad w_1^{(V)} \quad \dots \quad w_{m_V}^{(V)} \right). \quad (13)$$

For the K -classification problem, the regression coefficients corresponding to each discriminant function need to be determined, so a total of $K \times (KM)$ regression coefficients need to be determined. Considering that the coefficients corresponding to the same gene in each discriminant function should have the same weight, the weight vector \mathbf{w} should be repeated K times to obtain K identical row vectors, and these K identical row vectors



(a)

FIGURE 1: Continued.

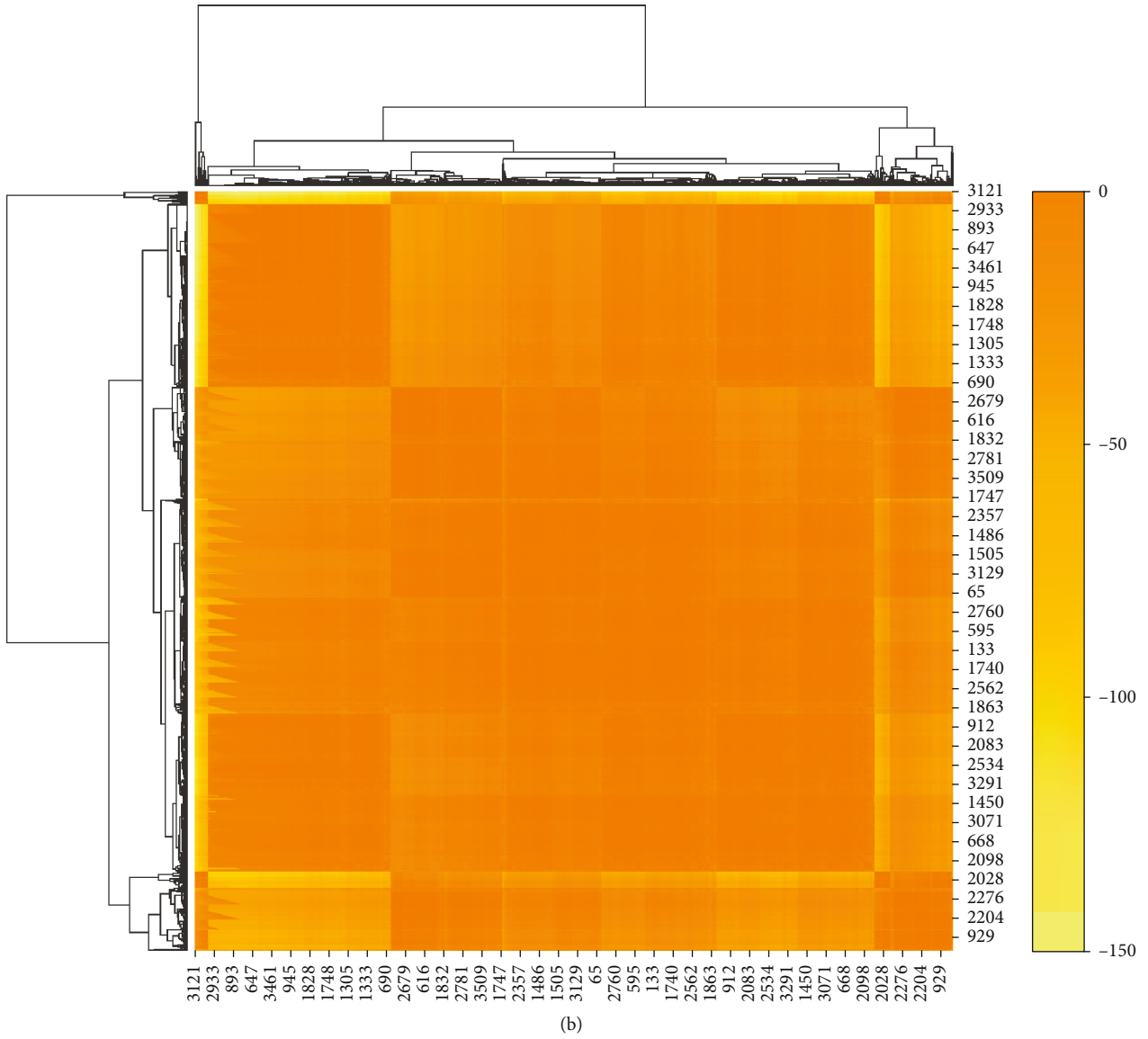


FIGURE 1: Continued.

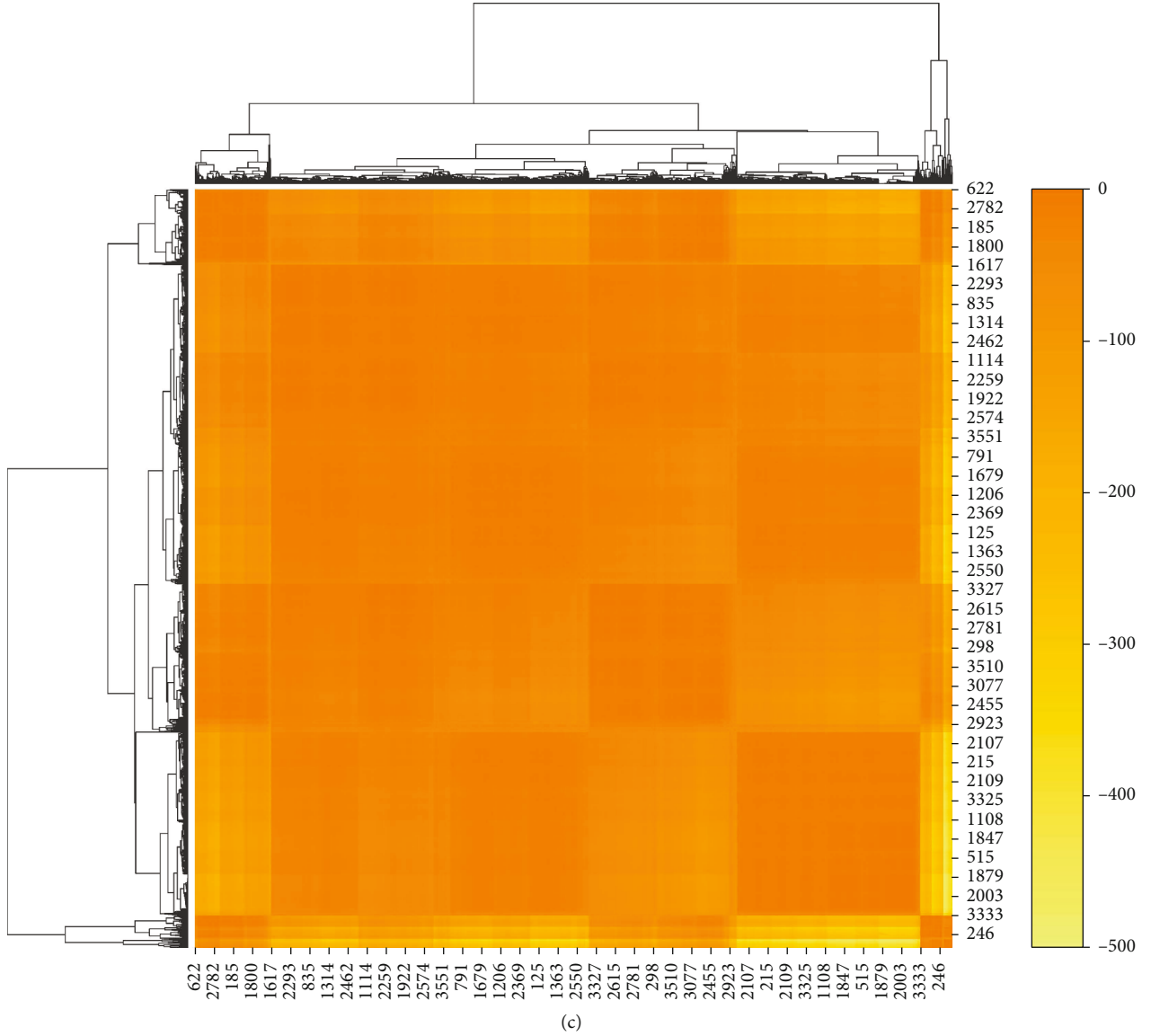


FIGURE 1: Heatmaps of AP clustering: (a) BALL, (b) TALL, and (c) AML.

can be combined by row to obtain the following K dimension weight matrix \mathbf{W} , i.e.,

$$\mathbf{W} = (\mathbf{w} \quad \mathbf{w} \quad \dots \quad \mathbf{w})^T. \quad (14)$$

By using noise information to evaluate the importance of each gene, the coefficients in the discriminant function can be adjusted adaptively. In this paper, we introduce the weight matrix \mathbf{W} into multiclass sparse groups Lasso penalty and establish the following model:

$$P_{(\alpha, \lambda)}(\beta) = (1 - \alpha)\lambda \sum_{k=1}^K \sum_{l=1}^V \sqrt{m_l} \|\beta_l^{(k)}\|_2 + \alpha\lambda \sum_{k=1}^K \left\| (\mathbf{W}\beta^T)_k \right\|_1, \quad (15)$$

where $\lambda \geq 0$ and $0 \leq \alpha \leq 1$ are the regularization parameters, $\beta = (\beta^{(1)}, \beta^{(2)}, \dots, \beta^{(K)})^T$ is the coefficient matrix, and $(\mathbf{W}\beta^T)_k$ is the k -th row of the matrix $\mathbf{W}\beta^T$.

The multinomial log-likelihood function does not need to presuppose the distribution of the data, and it can directly model the possibility of classification, so the loss function is used to estimate the empirical risk. By introducing adaptive multiclass sparse group Lasso penalty into multinomial log-likelihood function, this paper presents the following robust adaptive multinomial regression with sparse group Lasso penalty (RAMRSGL):

$$\min_{\beta_0, \beta} \left\{ -\frac{1}{n} \sum_{i=1}^n \left[\sum_{k=1}^K y_{ik} (\beta_0^{(k)} + \bar{\mathbf{x}}_i^T \beta^{(k)}) - \log \left(\sum_{k=1}^K e^{\beta_0^{(k)} + \bar{\mathbf{x}}_i^T \beta^{(k)}} \right) \right] + P_{(\alpha, \lambda)}(\beta) \right\}. \quad (16)$$

where $y_{ik} = I(y_i = k)$ is the indicator function, i.e., if the sample belongs to class k , $y_{ik} = 1$; otherwise, $y_{ik} = 0$.

For multiclassification problems, the penalty term $\sum_{k=1}^K \sum_{l=1}^V \sqrt{m_l} \|\beta_l^{(k)}\|_2$ enables RAMRSGL to select important gene groups for all discriminant functions. We also construct data-driven weights using the decomposed noise information, which enables adaptive gene selection within each group. At the same time, by introducing noise information into the model, the robustness of the model is further enhanced.

2.2.4. Solution Algorithm. Solving the group Lasso optimization problem is around for some time, e.g., Similä and Tikka [44] have developed an interesting application to multiresponse linear regression. Due to l_1 -norm penalty is not differentiable at the origin, group Lasso algorithms cannot be used to compute a solution to the sparse group Lasso optimization problem. Inspired by Vincent and Hansen [39], we also adopt the algorithm of block coordinate descent, comprising of the outer, middle, and inner coordinate descent loop.

In this work, the proposed RAMRSGL model is used to conduct multiclassification problem and gene selection on the gene expression data of multiple carcinomas. The specific steps are elaborated in Algorithm 1, which is implemented using the R language version of MSGSL toolkit (<https://github.com/nielsrhansen/msgsl>) proposed by Vincent and Hansen. The maximum iterations of the proposed RAMRSGL model are set to $i_{\max} = 1000$. Moreover, its convergence is proved theoretically, more details in [39].

Although AP clustering does not need to specify the number of clustering in advance, the final number of clustering is affected by the parameter of $p(i)$, which is the reference degree with the point i as clustering center. This means that the higher the value $p(i)$ is, the greater the possibility of this point becoming the clustering center is. For genes, since each data point has the same possibility of being the clustering center, all $p(i)$ is set to the same value, which is denoted as p .

3. Experiments

3.1. Dataset. The acute leukemia gene expression dataset is provided by Golub et al. [45], which contains 72 samples consisting of 7129 genes. According to [46], the diagnosis of acute leukemia can be considered as a tri-classification problem, with 38 samples of B-cell acute lymphoblastic leukemia (BALL), 9 samples of T-cell acute lymphoblastic leukemia (TALL), and 25 samples of acute myeloid leukemia (AML). Using the data preprocessing method in [45], 3571 important genes are selected preliminarily. In this paper, pre-processed data is used for the experiment, i.e., a dataset containing 72 samples of 3571 genes. The data is randomly divided into two parts, two-thirds for training and one-third for testing. In order to ensure the class balance of the data, 25 BALL samples, 6 TALL samples, and 17 AML samples are randomly selected as the training set, and the remaining 24 samples are used as the test set.

TABLE 1: Results of AP clustering on BALL, TALL, and AML.

Data	BALL	TALL	AML
Number of iterations	175	151	199
p value	-26.62758	-6.286937	-17.206
Sum of similarities	-3108.519	-449.0737	-2029.779
Net similarity	-4226.878	-675.4035	-2735.225
Number of clusters	42	36	41

TABLE 2: Performance of five methods on the leukemia dataset.

Methods	Average prediction accuracy	Average number of selected genes
RAMRSGL	0.958 (0.026)	52.2 (26.01)
AMRSGL	0.954 (0.043)	375.1 (119.66)
MRSGL	0.950 (0.036)	239.5 (122.20)
MRGL	0.954 (0.051)	571.7 (221.08)
l_1 -norm MR	0.946 (0.049)	21.7 (5.97)

TABLE 3: Classification accuracy and number of selected genes on the decomposed clean data.

Methods	Average prediction accuracy	Average number of selected genes
MRSGL	0.954 (0.039)	126.2 (34.25)
MRGL	0.958 (0.032)	160.2 (53.72)
l_1 -norm MR	0.958 (0.037)	18.9 (3.24)

3.2. Clustering Results. AP clustering is performed on BALL, TALL, and AML, respectively, and the heatmaps of AP clustering are shown in Figure 1. Table 1 elaborates the detailed results of AP clustering. According to the clustering strategy, take the default reference $p = -26.62758$ in BALL class. The 3571 genes are automatically divided into 42 clusters, among which the second cluster has the largest number of genes (252 genes), the first cluster has the smallest number of genes (22 genes), and most of the other clusters have about 100 genes. In TALL class, the default reference $p = -6.286937$ is taken, and the genes are automatically divided into 36 clusters. Among the 36 clusters, the number of genes varies greatly, with the largest cluster containing 347 genes and the smallest cluster containing only 17 genes. In AML class, the default reference $p = -17.206$ is taken, and the genes are divided into 41 clusters, with the largest containing 273 genes and the smallest containing 22 genes. Think of each cluster as a group, and each duplicated gene as a new gene. A total of 10713 genes are obtained by placing the 119 gene groups in a specific order. Table 1 also reports the fact iterations of the algorithm, from which it can be seen that AP clustering on all datasets can achieve convergence within a finite number of steps.

3.3. Performance Comparison. In this paper, the proposed RAMRSGL algorithm is compared with adaptive multinomial regression with sparse group Lasso (AMRSGL),

TABLE 4: Seven key genes selected by RAMRSL on leukemia data.

Gene	Number group	Gene title	Annotation of gene function
CDK1	2	Cyclin-dependent kinase 1	Phosphorylation and dephosphorylation of CDK1-encoded proteins play an important role in cell cycle regulation.
LRRC14	24, 65	Leucine-rich repeat containing 14	LRRC14 negatively regulates NF-kappa B transcription factor activity and toll-like receptor signaling pathway.
MIF	51	Macrophage migration inhibitory factor	MIF encodes a lymphokine involved in cell-mediated immunity, immunomodulation, and inflammation.
Srpr	84	Signal recognition particle receptor	Srpr plays a role in signal recognition of particle binding.
DGUOK	46	Deoxyguanosine kinase	The protein encoded by DGUOK is responsible for phosphorylation of purine DNA in the mitochondrial matrix.
SRI	88	Sorcin	SRI encodes a calcium-binding protein that regulates intracellular calcium homeostasis.
HSPB1	105	Heat shock protein family B member 1	HSPB1 encodes proteins that play important roles in the differentiation of a variety of cell types.

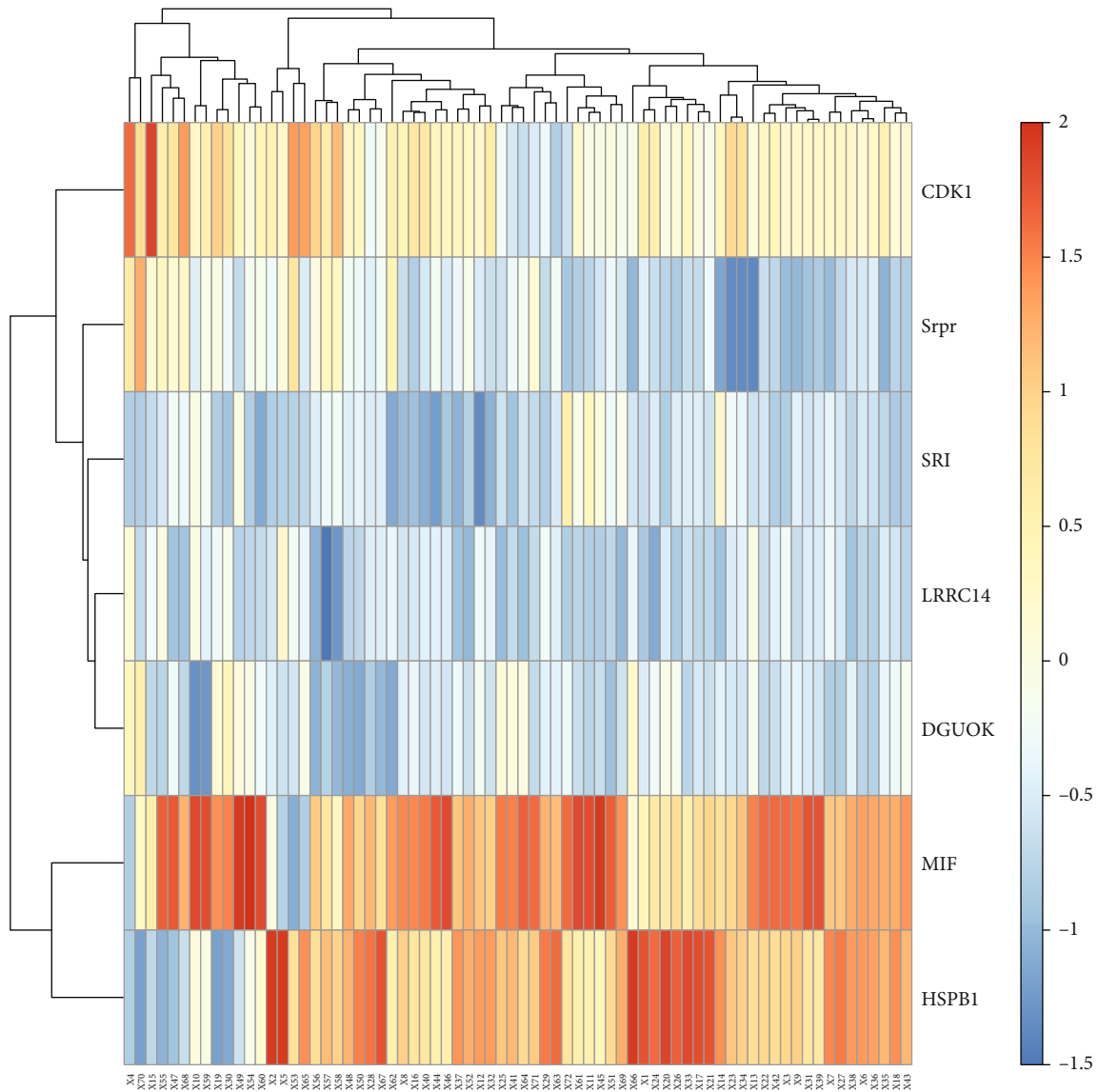


FIGURE 2: Clustering heat map of seven selected genes.

multinomial regression with sparse group Lasso penalty (MRSGL), multinomial regression with group Lasso penalty (MRGL), and multinomial regression with Lasso penalty (l_1 -norm MR). RAMRSGL is used to conduct experiments on the clean data obtained by decomposition, and the genes are clustered in advance by AP clustering. The other four methods are all tested on the original data. AMRSGL, MRSGL, and MRGL also used WGCNA for gene clustering, while l_1 -norm MR method does not require clustering in advance. The first three of the above methods have two model parameters α and λ that need to be determined. The last two have only one parameter λ to determine.

Table 2 presents the average classification accuracy and average number of selected genes of 10 experiments with different methods on the acute leukemia dataset, with standard deviation in brackets. As can be seen from Table 2, these five methods have achieved high classification accuracy, all reaching more than 94%. The proposed RAMRSGL method has the highest average classification accuracy, 95.8%, which is 0.4%, 0.8%, 0.4%, and 1.2% higher than the other four methods, respectively. AMRSGL and MRGL have achieved a suboptimal classification accuracy of 95.4%, and l_1 -norm MR has achieved the lowest classification accuracy of 94.6%. RAMRSGL achieved the smallest standard deviation, indicating that the method is more stable than other methods. It should be noted that the average number of selected genes varies greatly among the five methods. The MRGL method has the most genes selected, with an average number of 571.7. The average number of selected genes was only 21.7 by l_1 -norm MR method and 52.2 by RAMRSGL method. To sum up, the proposed RAMRSGL method has the highest classification accuracy and high simplicity, which makes the model easier to be interpreted.

In addition, to further illustrate the robustness of the proposed model and the effectiveness of AP clustering, the experimental results of the three methods on the decomposed clean data are presented in Table 3. Both MRSGL and MRGL use AP clustering to cluster genes in advance, while l_1 -norm MR does not cluster. The parameter selection method is consistent with the above. As can be seen from Table 3, the classification accuracy of these three methods on clean data is higher than before, and the variance is relatively small. It is proved that the use of robust principal component analysis can improve the model performance. Otherwise, the deviation of the prediction accuracy in Table 3 is higher than the proposed method in Table 2, which proves that the proposed method using AP clustering is more robust. In terms of gene selection, the experimental results of MRSGL and MRGL methods are significantly different from those of the previous ones, with the average number of selected genes being significantly reduced. The ability to achieve high accuracy with fewer genes is very attractive. After AP clustering is used for gene clustering in advance, fewer genes are selected by these methods, which may benefit from the fact that AP clustering can well reveal the group structure between genes, so as to achieve more accurate gene selection.

3.4. Gene Selection. In each experiment, as can be seen in Algorithm 1, we extract the nonzero coefficients β^* of the

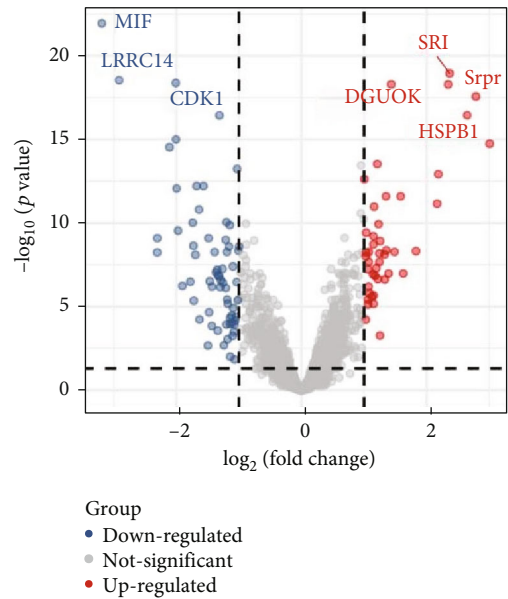


FIGURE 3: Volcano plot for differential expression of selected genes.

optimal model and determine the corresponding genes and groups. By selecting genes that appear 9 or more times in 10 experiments as key genes, RAMRSGL has identified 9 key genes on the leukemia dataset. Seven gene replicates are selected for 10 times, and two gene replicates are selected for 9 times. Table 4 lists seven genes and their corresponding group sequences that are present in each experiment. In addition, through the search of these genes in the NCBI database, the functional annotations of these 7 genes are also given in Table 4.

Figure 2 shows the heat map of the selected seven genes in different samples. It can be seen that genes HSPB1 and MIF have similar expressions in different samples and can be grouped into one group, while Srpr, SRI, DGUOK, and LRR14 can be grouped into another group. It is concluded that these genes have similar functions or are jointly involved in some gene pathways. Figure 3 illustrates the volcano plot for differential expression of 3571 genes where the differentially expressed genes are selected by the threshold $p < 0.05$ ($\log_2 FC < 1$ and $\log_2 FC > 1$). As can be seen from Figure 3, among the 7 screened genes, the expressions of SRI, Srpr, HSPB1, and DGUOK are significantly upregulated, while the expressions of MIF, LRR14, and CDK1 are significantly downregulated. The bubble diagram of genes selected in an experiment is shown in Figure 4. It can be seen from Figure 4 that the cell pathways involved in these genes mainly include viral myocarditis, tuberculosis, transcription disorders in cancer, hematopoietic cell lineage, and B cell signaling pathway. In addition, more of these genes are involved in cancer transcription disorders, and more are involved in viral infection.

Combined with gene function and literature, the relationship between five key genes and cancer is expounded.

3.4.1. DGUOK. The protein encoded by this gene is responsible for the phosphorylation of purine deoxyribonucleosides

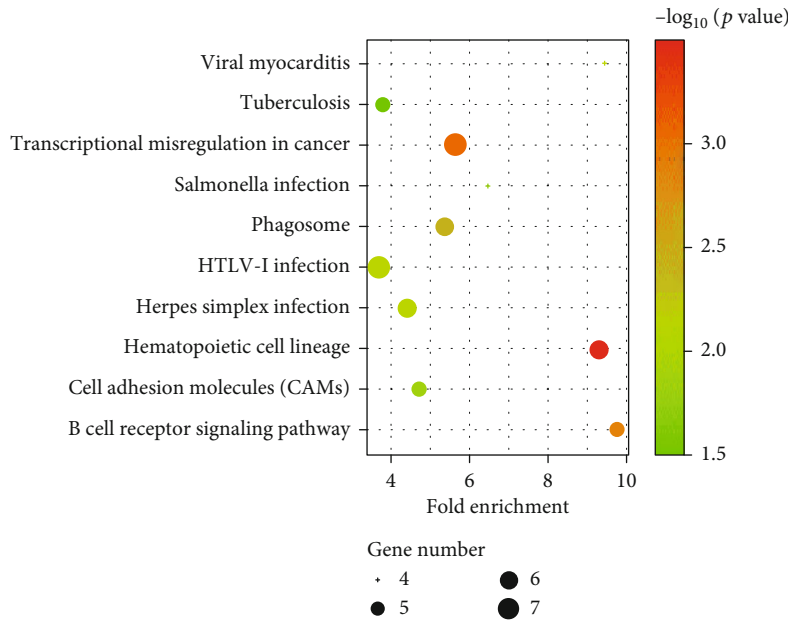


FIGURE 4: Bubble diagram of selected genes.

in the mitochondrial matrix. This protein phosphorylates several purine deoxyribonucleoside analogs used in the treatment of lymphoproliferative disorders, and this phosphorylation is critical for the effectiveness of the analogs. Wu et al. [47] have found that DGUOK-AS1 is upregulated in cervical squamous cell carcinoma and intracervical adenocarcinoma (CESC) tissues. Their research has also shown that DGUOK-AS1 is highly expressed in liver cancer cell lines and can promote the proliferation of cervical cancer cells by releasing EMSY as the ceRNA of miR-653-5p.

3.4.2. *MIF*. This gene encodes a lymphokine involved in cell-mediated immunity, immune regulation, and inflammation. By inhibiting the anti-inflammatory effects of glucocorticoids, it regulates the function of macrophages in host defense. Osipyan et al. [48] have found that MIF can trigger the mitogen-activated protein kinase and phosphoinositic acid 3-kinase signaling pathways by binding to CD74 and other receptors. The change in the expression value of MIF and changes in the active state of connection pathways are related to inflammatory diseases and cancer.

3.4.3. *CDK1*. The protein encoded by this gene is a member of the Ser/Thr protein kinase family. This protein is the catalytic subunit of the highly conserved protein kinase complex M-phase promoting factor (MPF), which plays an important role in the transition of the G1/S and G2/M phases of the eukaryotic cell cycle. The mitotic cyclin binds to the protein stably and functions as a regulatory subunit. The phosphorylation and dephosphorylation of this protein also play an important regulatory role in cell cycle control. Huang et al. [49] have studied the mechanism of CDK1 in lung cancer and found that CDK1 is regulated by NF- κ B through a hypothetical κ B site in its proximal promoter.

3.4.4. *Srpr*. This gene encodes a subunit of the endoplasmic reticulum signal recognition particle receptor, and together with the signal recognition particle, it participates in the targeting and translocation of secreted proteins and cell membrane proteins marked by signal sequences. Alternative splicing leads to multiple transcriptional variations. Kim et al. [50] have found that *Srpr* is highly expressed in epidermal keratinocytes and regulates the proliferation of keratinocytes by affecting cell cycle progression.

3.4.5. *HSPB1*. This gene encodes a protein of the small heat shock protein (HSP20) family. This protein plays an important role in the differentiation of many cell types. The expression of this gene is associated with the adverse clinical outcomes of a variety of human cancers. The encoded protein can promote the proliferation and metastasis of cancer cells, while protecting cancer cells from apoptosis. Rajesh et al. [51] have established Fli-1 (Fli-1), a member of the Ets family, which plays a transcriptional regulatory role on the *HSPB1* gene. Fli-1 binds to the nucleotide residues GGAA at binding sites 3, 6, and 7 in the 5-kb region upstream of *HSPB1*. Fli-1 is related to oncogenic transformation and upregulation in radio/TMZR GBM.

4. Conclusions

In this paper, a robust adaptive multinomial regression model with sparse group Lasso penalty is proposed and its solution algorithm is developed, based on robust principal component analysis and AP clustering with overlapping strategy. The proposed method is applied to the diagnosis of triple-cancer leukemia, and the accuracy of diagnosis is up to 95.8%, which is better than other state-of-the-art methods. In addition, seven key genes are screened out, and the relationship between five key genes and cancer is

expounded in combination with gene function and relative literature. In the future, the nonlinear problem will be studied.

Data Availability

The acute leukemia gene expression dataset is provided by Golub et al., which can be download at <https://www.kaggle.com/crawford/gene-expression>.

Conflicts of Interest

The authors declare that there is no conflict of interest regarding the publication of this paper.

Acknowledgments

This work was supported by the Natural Science Foundation of China (61203293, 31700858) and the Scientific and Technological Project of Henan Province (212102210140).

References

- [1] J. Zhao, C. Leng, L. Li, and H. Wang, "High-dimensional influence measure," *The Annals of Statistics*, vol. 41, no. 5, pp. 2639–2667, 2013.
- [2] Q. Mai, H. Zou, and M. Yuan, "A direct approach to sparse discriminant analysis in ultra-high dimensions," *Biometrika*, vol. 99, no. 1, pp. 29–42, 2012.
- [3] L. Chen, Y. H. Zhang, G. Lu, T. Huang, and Y. D. Cai, "Analysis of cancer-related lncRNAs using gene ontology and KEGG pathways," *Artificial Intelligence in Medicine*, vol. 76, pp. 27–36, 2017.
- [4] L. Chen, J. Li, and M. Chang, "Cancer diagnosis and disease gene identification via statistical machine learning," *Current Bioinformatics*, vol. 15, no. 9, pp. 956–962(7), 2020.
- [5] L. Chen, T. Zeng, X. Pan, Y.-H. Zhang, T. Huang, and Y.-D. Cai, "Identifying methylation pattern and genes associated with breast cancer sub-types," *International Journal of Molecular Sciences*, vol. 20, no. 17, p. 4269, 2019.
- [6] L. Chen, X. Pan, X. H. Hu et al., "Gene expression differences among different MSI statuses in colorectal cancer," *International Journal of Cancer*, vol. 143, no. 7, pp. 1731–1740, 2018.
- [7] K. Kourou, T. P. Exarchos, K. P. Exarchos, M. V. Karamouzis, and D. I. Fotiadis, "Machine learning applications in cancer prognosis and prediction," *Computational and Structural Biotechnology Journal*, vol. 13, pp. 8–17, 2015.
- [8] Y. Saeys, I. Inza, and P. Larranaga, "A review of feature selection techniques in bioinformatics," *Bioinformatics*, vol. 23, no. 19, pp. 2507–2517, 2007.
- [9] M. Mokhtaridoost and M. Gönen, "Identifying key miRNA-mRNA regulatory modules in cancer using sparse multivariate factor regression," in *International Conference on Machine Learning, Optimization, and Data Science*, pp. 422–433, Springer, 2020.
- [10] X. Zhang, Q. Zhang, X. Wang, S. Ma, and K. Fang, "Structured sparse logistic regression with application to lung cancer prediction using breath volatile biomarkers," *Statistics in Medicine*, vol. 39, no. 7, pp. 955–967, 2020.
- [11] Q. Zhang, J. Zhou, and B. Zhang, "A noninvasive method to detect diabetes mellitus and lung cancer using the stacked sparse autoencoder," in *ICASSP 2020 - 2020 IEEE International Conference on Acoustics, Speech and Signal Processing (ICASSP)*, pp. 1409–1413, Barcelona, Spain, May 2020.
- [12] Z. Y. Algamal and M. H. Lee, "A two-stage sparse logistic regression for optimal gene selection in high-dimensional microarray data classification," *Advances in Data Analysis and Classification*, vol. 13, no. 3, pp. 753–771, 2019.
- [13] S. Wu, H. Jiang, H. Shen, and Z. Yang, "Gene selection in cancer classification using sparse logistic regression with l1/2 regularization," *Applied Sciences*, vol. 8, no. 9, p. 1569, 2018.
- [14] M. Yuan and Y. Lin, "Model selection and estimation in regression with grouped variables," *Journal of the Royal Statistical Society: Series B (Statistical Methodology)*, vol. 68, no. 1, pp. 49–67, 2006.
- [15] H. Zhang, J. Wang, Z. Sun, J. M. Zurada, and N. R. Pal, "Feature selection for neural networks using group lasso regularization," *IEEE Transactions on Knowledge and Data Engineering*, vol. 32, no. 4, pp. 659–673, 2019.
- [16] Z. Zhao, S. Wu, B. Qiao, S. Wang, and X. Chen, "Enhanced sparse period-group lasso for bearing fault diagnosis," *IEEE Transactions on Industrial Electronics*, vol. 66, no. 3, pp. 2143–2153, 2018.
- [17] G. Xie, C. Dong, Y. Kong, J. F. Zhong, M. Li, and K. Wang, "Group lasso regularized deep learning for cancer prognosis from multi-omics and clinical features," *Genes*, vol. 10, no. 3, p. 240, 2019.
- [18] N. Simon, J. Friedman, T. Hastie, and R. Tibshirani, "A sparse-group lasso," *Journal of Computational and Graphical Statistics*, vol. 22, no. 2, pp. 231–245, 2013.
- [19] J. Li, Y. Wang, X. Song, and H. Xiao, "Adaptive multinomial regression with overlapping groups for multi-class classification of lung cancer," *Computers in Biology and Medicine*, vol. 100, pp. 1–9, 2018.
- [20] M. B. Eisen, P. T. Spellman, P. O. Brown, and D. Botstein, "Cluster analysis and display of genome-wide expression patterns," *Proceedings of the National Academy of Sciences*, vol. 95, no. 25, pp. 14863–14868, 1998.
- [21] D. Chaussabel and N. Baldwin, "Democratizing systems immunology with modular transcriptional repertoire analyses," *Nature Reviews Immunology*, vol. 14, no. 4, pp. 271–280, 2014.
- [22] J. Kim, R. Krishnapuram, and R. Davé, "Application of the least trimmed squares technique to prototype-based clustering," *Pattern Recognition Letters*, vol. 17, no. 6, pp. 633–641, 1996.
- [23] J. Hämmäläinen, S. Jauhiainen, and T. Kärkkäinen, "Comparison of internal clustering validation indices for prototype-based clustering," *Algorithms*, vol. 10, no. 3, p. 105, 2017.
- [24] L. McInnes, J. Healy, and S. Astels, "hdbscan: hierarchical density based clustering," *Journal of Open Source Software*, vol. 2, no. 11, p. 205, 2017.
- [25] R. J. Campello, P. Kröger, J. Sander, and A. Zimek, "Density-based clustering," *WIREs Data Mining and Knowledge Discovery*, vol. 10, no. 2, article e1343, 2020.
- [26] V. Cohen-addad, V. Kanade, F. Mallmann-trenn, and C. Mathieu, "Hierarchical clustering: objective functions and algorithms," *Journal of the ACM*, vol. 66, no. 4, pp. 1–42, 2019.
- [27] A. K. Dutta, M. Elhoseny, V. Dahiya, and K. Shankar, "An efficient hierarchical clustering protocol for multihop internet of vehicles communication," *Transactions on Emerging Telecommunications Technologies*, vol. 31, no. 5, article e3690, 2020.

- [28] X. Yang, C. Deng, F. Zheng, J. Yan, and W. Liu, "Deep spectral clustering using dual autoencoder network," in *2019 IEEE/CVF Conference on Computer Vision and Pattern Recognition (CVPR)*, pp. 4066–4075, Long Beach, CA, USA, June 2019.
- [29] R. Sharan, A. Maron-Katz, and R. Shamir, "CLICK and expander: a system for clustering and visualizing gene expression data," *Bioinformatics*, vol. 19, no. 14, pp. 1787–1799, 2003.
- [30] B. Zhang and S. Horvath, "A general framework for weighted gene co-expression network analysis," *Statistical Applications in Genetics and Molecular Biology*, vol. 4, no. 1, 2005.
- [31] B. J. Frey and D. Dueck, "Clustering by passing messages between data points," *Science*, vol. 315, no. 5814, pp. 972–976, 2007.
- [32] Y. Chen, C. Caramanis, and S. Mannor, "Robust sparse regression under adversarial corruption," in *Proceedings of the 30th International Conference on Machine Learning, PMLR*, pp. 774–782, Atlanta, GA, USA, 2013.
- [33] A. Wahid, D. M. Khan, and I. Hussain, "Robust adaptive lasso method for parameter's estimation and variable selection in high-dimensional sparse models," *PLoS One*, vol. 12, no. 8, article e0183518, 2017.
- [34] H. Yang and N. Li, "WLAD-LASSO method for robust estimation and variable selection in partially linear models," *Communications in Statistics-Theory and Methods*, vol. 47, no. 20, pp. 4958–4976, 2018.
- [35] N. H. Nguyen and T. D. Tran, "Robust lasso with missing and grossly corrupted observations," *IEEE Transactions on Information Theory*, vol. 59, no. 4, pp. 2036–2058, 2012.
- [36] H. Wang, G. Li, and G. Jiang, "Robust regression shrinkage and consistent variable selection through the lad-lasso," *Journal of Business & Economic Statistics*, vol. 25, no. 3, pp. 347–355, 2007.
- [37] S. Lambert-Lacroix and L. Zwald, "Robust regression through the Huber's criterion and adaptive lasso penalty," *Electronic Journal of Statistics*, vol. 5, pp. 1015–1053, 2011.
- [38] Q. Zheng, C. Gallagher, and K. B. Kulasekera, "Robust adaptive lasso for variable selection," *Communications in Statistics-Theory and Methods*, vol. 46, no. 9, pp. 4642–4659, 2017.
- [39] M. Vincent and N. R. Hansen, "Sparse group lasso and high dimensional multinomial classification," *Computational Statistics & Data Analysis*, vol. 71, pp. 771–786, 2014.
- [40] J.-P. Zhou, L. Chen, and Z. H. Guo, "iATC-NRAKEL: an efficient multi-label classifier for recognizing anatomical therapeutic chemical classes of drugs," *Bioinformatics*, vol. 36, no. 5, pp. 1391–1396, 2019.
- [41] J.-P. Zhou, L. Chen, T. Wang, and M. Liu, "iATC-FRAKEL: a simple multi-label web server for recognizing anatomical therapeutic chemical classes of drugs with their fingerprints only," *Bioinformatics*, vol. 36, no. 11, pp. 3568–3569, 2020.
- [42] R. Tibshirani, "Regression shrinkage and selection via the lasso," *Journal of the Royal Statistical Society: Series B (Methodological)*, vol. 58, no. 1, pp. 267–288, 1996.
- [43] E. J. Candès, X. Li, Y. Ma, and J. Wright, "Robust principal component analysis?," *Journal of the ACM*, vol. 58, no. 3, pp. 1–37, 2011.
- [44] T. Similä and J. Tikka, "Input selection and shrinkage in multi-response linear regression," *Computational Statistics & Data Analysis*, vol. 52, no. 1, pp. 406–422, 2007.
- [45] T. R. Golub, D. K. Slonim, P. Tamayo et al., "Molecular classification of cancer: class discovery and class prediction by gene expression monitoring," *Science*, vol. 286, no. 5439, pp. 531–537, 1999.
- [46] Y. Lee and C. K. Lee, "Classification of multiple cancer types by multicategory support vector machines using gene expression data," *Bioinformatics*, vol. 19, no. 9, pp. 1132–1139, 2003.
- [47] N. Wu, H. Song, Y. Ren, S. Tao, and S. Li, "DGOOK-AS1 promotes cell proliferation in cervical cancer via acting as a ceRNA of mir-653-5p," *Cell Biochemistry and Function*, vol. 38, no. 7, pp. 870–879, 2020.
- [48] A. Osipyan, D. Chen, and F. J. Dekker, "Epigenetic regulation in macrophage migration inhibitory factor (MIF)-mediated signaling in cancer and inflammation," *Drug Discovery Today*, 2021.
- [49] Z. Huang, G. Shen, and J. Gao, "Cdk1 promotes the stemness of lung cancer cells through interacting with sox2," *Clinical and Translational Oncology*, 2021.
- [50] B.-K. Kim, H. I. Yoo, K. Choi, A. R. Lee, and S. K. Yoon, "Regulation of srpr expression by mir-330-5p controls proliferation of mouse epidermal keratinocyte," *PLoS One*, vol. 11, no. 10, article e0164896, 2016.
- [51] Y. Rajesh, A. Biswas, P. Banik et al., "Transcriptional regulation of hspb1 by friend leukemia integration-1 factor modulates radiation and temozolomide resistance in glioblastoma," *Oncotarget*, vol. 11, no. 13, pp. 1097–1108, 2020.